Estonian Journal of Engineering, 2011, **17**, 1, 66–75 doi: 10.3176/eng.2011.1.07

Axial defect imaging in a pipe using synthetically focused guided waves

Madis Ratassepp[a], Sam Fletcher[b] and Aleksander Klauson[a]

[a] Department of Mechanics, Tallinn University of Technology, Ehitajate tee 5, 19086 Tallinn, Estonia; madis.ratassepp@ttu.ee
[b] Department of Mechanical Engineering, Imperial College, London SW7 2BX, United Kingdom

Received 26 October 2010, in revised form 10 January 2011

Abstract. Ultrasonic guided waves have been recognized as an effective tool for a rapid, long-range inspection of pipes. Still this technique has several difficulties in locating and quantifying defects properly due to the complex nature of guided waves. In this study a defect imaging technique is implemented to detect axially aligned defects in pipes. Imaging is necessary to locate the defect position and to improve the reflection coefficient from axially aligned defects, as the signals are very weak. The common source method of synthetic focusing has been applied, which makes it possible to determine information of the defect from the reconstructed image. By using data from finite element modelling, the dependence of the reflection coefficient on crack length was measured for both through thickness and part depth axially aligned defects at a range of frequencies, using the torsional guided wave family. The results show that the reflection coefficient is increased when focusing is employed, compared to unfocused fundamental torsional waves. However, the sensitivity is still very low, thus in practice this approach could only be used to find severe defects.

Key words: pipes, axial crack, ultrasonic guided waves, defect imaging.

1. INTRODUCTION

Nondestructive testing (NDT) with ultrasonic guided waves has become a well established long range inspection procedure for pipes [1,2]. In this application tens of metres of the structure can be remotely screened for defects from a single test location which is far more efficient than the tedious and time-consuming conventional point-by-point scanning methods, and it is possible to perform inspection of inaccessible locations. The basic idea of the technique is that the presence of the defect in the wall of the pipe causes the scattering of the guided wave. The measurement of these scattered waves can thus enable defect detection and characterization.

The investigation of the potential of guided waves for the detection of defects in pipes has been intense [1–8]. Axisymmetric guided wave modes have been mainly used for the screening of long pipe sections to detect defects. Both, low frequency longitudinal wave mode L(0,2) [3] and torsional wave mode T(0,1) [4] have been found to be good candidates for such testing as their wave fields allow to achieve 100% pipe wall inspection coverage and due to non-dispersive nature their wave pulses can propagate long distances. In such systems it is possible to predict the axial position of the defect by measuring arrival time of the reflected wave modes. The severity of the defect can be estimated by measuring the reflection amplitude. However, it is not possible to determine the circumferential position of the defect and also the sizing of small circumferential defects is problematic [4,5]. Previous research by the authors [6] examined the reflection of the torsional guided wave mode T(0,1) from an axial crack in a pipe. The research showed that it was possible to detect an axial crack only in ideal circumstances; in practice, provided the crack extended through 80% of the wall thickness. One solution to increase the inspection sensitivity in this case is to use focusing. Recently, the synthetic focusing technique has been proposed [7,8] in which the location and other parameters of the defect can be determined directly from the reconstructed pipe image. The technique is based on post-processing of the recorded backscattered defect signals, which are time-reversed to form an image of the defect in the pipe wall. It has been demonstrated that by focusing the guided waves it should be possible to increase the reflection amplitude, compared to unfocused guided waves [8], which could be helpful also in the detection of an axial crack.

In this paper we implement a defect imaging technique to locate and quantify an axial crack in a pipe when the torsional mode T(0,1) is excited. A short description of the pipe imaging method is given and the algorithm is tested by finite element modelling. The paper focuses on the analysis of the reflection as a function of length, depth, diameter of the pipe and frequency of the incident signal.

2. IMAGING PROCEDURE

Consider a pipe shown in Fig. 1. The shear transducers, aligned circumferentially around the pipe end A, are excited simultaneously to produce a fundamental torsional T(0,1) guided wave mode. The interaction of the excited wave mode with an axial crack and pipe end B causes reflections, which are monitored independently with each receiving transducer. The imaging is performed by the common source method (CSM) as it has been found to be the most appropriate technique for pipe imaging [9].

The recorded circumferential displacement time series at the coordinate $z = 0$ are organized into a data matrix $v(z = 0, \theta, t)$, depending on time t and circumferential position θ. Next step is to decompose the recorded wave field

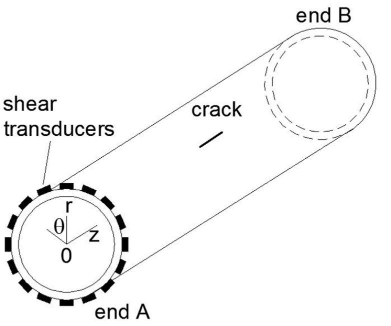

Fig. 1. Schematic set-up for defect imaging in a pipe.

into its circumferential modal components with index n at different angular frequencies ω. This is performed by double Fourier transform over t and θ

$$V(z=0,n,\omega)=\int_{-\infty}^{\infty}\int_{-\infty}^{\infty}v(z=0,\theta,t)e^{-in\theta}e^{-i\omega t}\mathrm{d}\theta\mathrm{d}t, \tag{1}$$

where $V(z=0,n,\omega)$ represents the decomposition of the recorded reflected field into the torsional-flexural mode family (T(0,1), F(1,2), ... , F(n,2)) [8]. Each mode is back-propagated separately by spatial phase shifting the decomposition to an axial location at $z=z_1$ as follows

$$V(z_1,n,\omega)=V(z=0,n,\omega)e^{-i\xi_0 z_1}e^{-i\xi_n z_1}, \tag{2}$$

where ξ_0 accounts for the wavenumber of the incident T(0,1) mode and ξ_n for the reflected wave mode. Here it is important to note that the wavenumber can be approximated with plate solutions to ensure sufficient accuracy as shown in [8]. The reconstructed image at $z=z_1$ is the inverse spatial Fourier transform over summed phase shifted decompositions

$$I(z=z_1,\theta)=\frac{1}{(2\pi)^2}\int_{-\infty}^{\infty}\int_{-\infty}^{\infty}V(z=z_1,n,\omega)e^{i\omega t}e^{in\theta}\mathrm{d}\omega\mathrm{d}n. \tag{3}$$

The result is a 3D image of an unrolled pipe display. An example image, produced from finite element data, is shown in Fig. 2a. The defect is a through thickness axial crack with a length of 28 mm. The centre frequency of the tone burst is 60 kHz. The image shows the defect at the correct location at 1.8 m and the end wall at 3.7 m. Figure 2b shows the axial crack and pipe end wall image profiles at the crack plane. The image amplitude is scaled to the undamaged pipe end wall image amplitude. The defect image is characterized by its full width at the half of the maximum amplitude in axial ($\mathrm{FWHM_z}$) and cirumferential ($\mathrm{FWHM_\theta}$) direction.

The performance of the focusing method can be quantified as the amplitude gain and the improvement in sizing ability over the unfocused system. The

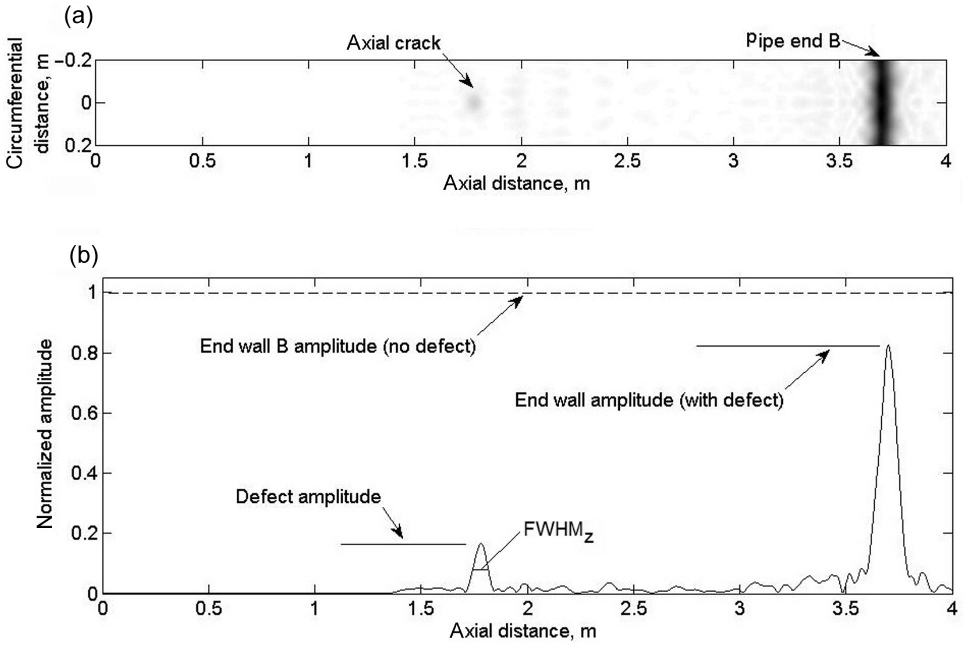

Fig. 2. (a) Unrolled pipe display image using finite element data at 60 kHz: 28 mm long through-thickness axial crack at 1.8 m and pipe end wall B at 3.7 m; (b) axial image profiles of the defect and pipe end wall in the crack plane.

amplitude from the unfocused method can be calculated by simply summing up the time traces, recorded at each transducer around the circumference [5]

$$F(n, z=0, t) = \sum\nolimits_{\theta} v(z=0, \theta, t) e^{n\theta/2\pi}. \tag{4}$$

In this work only the results for the mode $n = 0$, which corresponds to the fundamental guided mode T(0,1), are presented.

3. FINITE ELEMENT MODELLING

The interaction of the T(0,1) mode with circumferential and axial cracks has been successfully studied in the past using the finite element method (FEM) [4,6]. The FEM analysis was conducted using the ABAQUS software with its explicit time stepping procedure [10]. Membrane models with through-thickness cracks and 3D pipe models with part-depth cracks were used for this study. The length of the pipe was 3.7 m, its middle radius 64 mm and thickness 12.7 mm. The material of the pipe was steel (Young modulus $E = 210$ GPa, Poisson ratio $\nu = 0.3$ and density $\rho = 7900$ kg/m^3).

In the membrane model, the pipe mesh was created by linear four noded quadrilateral membrane elements representing the single pipe layer in the centre of the pipe thickness. It consisted of 925 elements along the length and 128 elements around the circumference, thus the resulting element size satisfied the lower limit of eight elements per wavelength, respecting the spatial discretization limit required for accurate modelling [5]. Additionally, some larger radius pipes were modelled by using more elements with the same element dimensions along the circumference. Zero-width cracks with zero stress on edges were modelled by disconnecting adjacent elements. The length of the crack was varied from 8 to 260 mm.

In the 3D model, the whole volume of the pipe was discretisized using eight-node "brick" elements. Similarly to the membrane model, 925 elements were used along the pipe length, 128 elements around the circumference and additionally 5 elements through the wall thickness. The cracks were modelled on the outer surface 40%, 60% and 80% deep through the wall thickness.

In both models the axisymmetric torsional mode T(0,1) was generated by prescribing identical circumferential displacement time histories on the outer surface at all nodes at the end A of the pipe. The test signal was 5-cycle tone burst, modulated by Hanning window. For each crack length, the central frequency of excitation was varied from 15 to 60 kHz. The detection of reflected waves was achieved simply by monitoring at 16 nodes, simulating the receivers, equally spaced around the circumference at the end A of the pipe, which corresponds to practical situation [6].

4. RESULTS AND DISCUSSION

4.1. Reflection amplitude as a function of crack length, frequency and pipe size

The variation of the reflection amplitude, with axial length of the through-thickness crack normalized to incident wavelength, is shown in Fig. 3. The centre frequency of the incident wave T(0,1) is varied from 15 to 60 kHz. The curves represent the processed FEM data by CSM and unfocused guided wave method. The peaks and troughs in the curves are due to interference of reflection components from the crack, as was explained in [6]. It is clear from a comparison of the focused and non-focused method results that employing focusing leads to an increased reflection amplitude when the frequency increases. At 15 kHz the results are overlapping but at 60 kHz the advantage of focusing over non-focusing is remarkable. A similar result was obtained in [9], where imaging of circular cracks in pipes was performed and the increase in sensitivity at higher inspection frequencies was observed. The reason for such improvement is that the non-focusing method considers only the reflection of T(0,1) guided wave mode while the focusing of guided waves takes into account all the reflected torsional-flexural guided wave modes, which amplitudes are summed up in the CSM imaging algorithm. As the axial crack is a non-axisymmetric feature in a pipe, the mode conversions take place to the F(n,2) modes, which contribute to

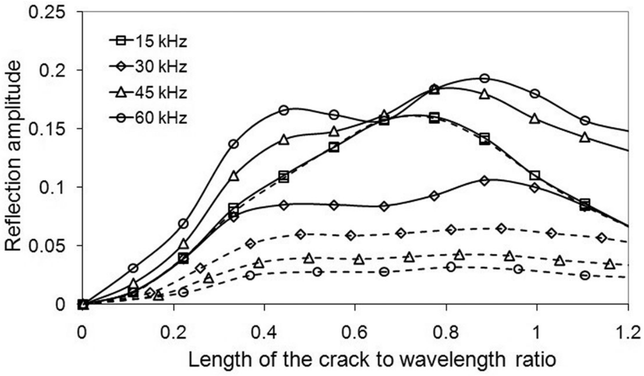

Fig. 3. Variation of the reflection amplitude with the length of the through-thickness crack; solid lines – results with CSM; dashed lines – results with unfocused guided waves.

the image amplitude. Moreover, when the frequency increases, higher circumferential order guided modes can propagate in the pipe, amplifying the image amplitude of the crack.

Figure 4 shows the reflection amplitude as a function of pipe circumference, which is normalized to the incident wavelength. The simulations are performed for a 36 mm long crack at 35 kHz. It is known that by using non-focusing method the reflection amplitude from an axial crack is inversely proportional to the pipe circumference [6], which is also seen in the figure. However, the curve obtained by CSM is rising after 4 wavelengths. A similar phenomenon of mode-conversions to higher circumference order modes occurs as the pipe size increases and therefore the amplitude of the image increases. Note that the CSM curve does not rise indefinitely but approaches the greatest possible theoretical amplitude, which can be calculated from the results of the non-focused method [8].

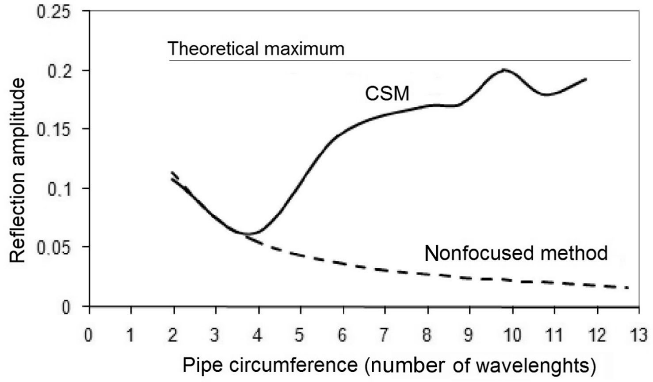

Fig. 4. Variation of the reflection amplitude with pipe circumference; the crack length was 36 mm and the incident wave was generated at 35 kHz.

4.2. Dependence on the crack depth

The variation of the reflection amplitude from an 80% deep axial crack in a pipe is shown in Fig. 5 for a range of crack lengths and frequencies. Again, the advantage of using the CSM method over the nonfocusing method can be observed by higher frequencies. The largest reflection amplitudes are obtained at 60 kHz.

Figure 6 shows the reflection amplitude as a function of the crack depth for the CSM method. A crack length of 0.37 wavelengths of the incident wave was selected as it produces the signals with highest amplitudes, with these results consequently being a "best-case" scenario. The results show that the reflection amplitude drops when the crack depth decreases. However, there is a difference between two curves obtained at 35 and 60 kHz. It can be seen that at lower frequencies the curve drops much faster, suggesting that it is more difficult to detect shallower defects as the test frequency is decreased.

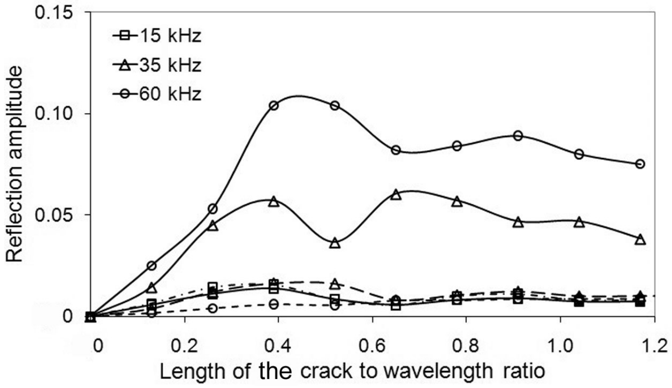

Fig. 5. Variation of the reflection amplitude with length of an 80% deep crack; solid lines – results with CSM, dashed lines – results with unfocused guided waves.

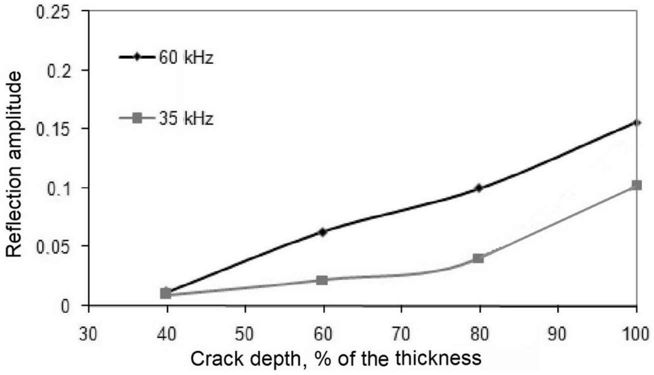

Fig. 6. Results from CSM showing the variation of the reflection amplitude with crack depth. The crack length was 20 mm at 60 kHz, and 36 mm at 35 kHz.

In good conditions, the on-site reflection amplitude of 0.05 would generally be considered the limit of detectability. This means that by using 60 kHz, a 60% deep crack could be detected, which is already a very severe defect.

4.3. Crack size estimation

Figure 7 shows the images of FWHM_z and FWHM_θ from finite element predictions, plotted against crack axial length at 35 kHz. It can be seen that both parameters are not affected much by the crack length. It is well known, according to the classical diffraction limit, that the conventional imaging systems are not capable to size features that are smaller than one wavelength of the probing wave. As the circumferential width of the crack is smaller than a wavelength then the measured FWHM_θ gives only an estimate that the defect width can be within a wavelength range. Similarly the length of the crack cannot be measured by FWHM_z as it is constantly around 1.5 wavelengths of the incident mode for all crack lengths. Therefore the direct length and depth estimation from the image parameters is not possible. Only the amplitude of the image can give some information of the crack. Figure 5 shows that the first peak amplitude of the reflection occurred around crack lengths of 0.4 wavelengths of the incident wave. Obtaining the variation of the frequency peak reflection versus crack length can potentially provide information about the crack length by identifying the frequency of the maximum reflection. The depth of the crack can be then determined from the absolute reflection amplitude from Fig. 6. Therefore, in practice it is necessary to test at several central frequencies.

5. CONCLUSIONS

An attempt has been made to use imaging to locate and quantify axially aligned defects in pipes. The need for imaging arises because standard guided wave techniques are not able to measure circumferential position of the defects and they are not sufficiently sensitive to axial defects in pipes. Focusing the

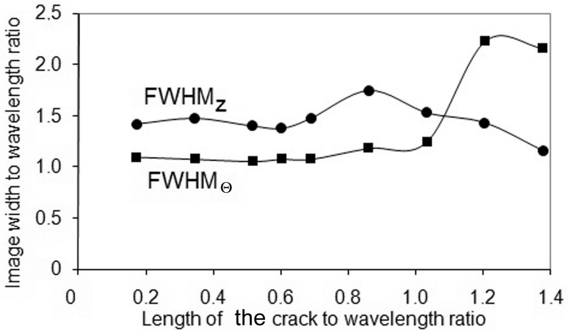

Fig. 7. The FWHM of the axial crack image against crack axial length in incident wavelengths.

guided waves, using the common source method, was employed on data from finite element models. It was discovered that focusing does improve the reflection amplitude from an axial defect compared to conventional nonfocusig guided wave technique. The increase in reflection amplitude has been attributed to taking into account all of the flexural-torsional modes, scattered from a defect. The study shows that the method can detect only severe defects and the sizing of the crack can be performed by analysing the change of the peak frequency of the reflection amplitude spectrum.

ACKNOWLEDGEMENTS

Madis Ratassepp and Aleksander Klauson are grateful to the Estonian Ministry of Education and Research (grant No. SF0140072s08) and Estonian Science Foundation (grant No. 7900) for supporting this work.

REFERENCES

1. Alleyne, D. N. and Cawley, P. Long range propagation of Lamb waves in chemical plant pipework. *Mater. Eval.*, 1997, **55**, 504–508.
2. Alleyne, D. N., Pavlakovic, B., Lowe, M. J. S. and Cawley, P. Rapid, long range inspection of chemical plant pipework using guided waves. *Insight*, 2001, **43**, 93–96.
3. Alleyne, D. N., Lowe, M. J. S. and Cawley, P. The reflection of guided waves from circumferential notches in pipes. *J. Appl. Mech.*, 1998, **65**, 635–641.
4. Demma, A., Cawley, P. and Lowe, M. J. S. The reflection of the fundamental torsional mode from cracks and notches in pipes. *J. Acoust. Soc. Am.*, 2003, **114**, 611–625.
5. Lowe, M. J. S., Alleyne, D. N. and Cawley, P. The mode conversion of a guided wave by a part-circumferential notch in a pipe. *J. Appl. Mech.*, 1998, **65**, 649–656.
6. Ratassepp, M., Fletcher, S. and Lowe, M. J. S. Scattering of the fundamental torsional mode at an axial crack in a pipe. *J. Acoust. Soc. Am.*, 2010, **127**, 730–740.
7. Hayashi, T. and Murase, M. Defect imaging with guided waves in a pipe. *J. Acoust. Soc. Am.*, 2005, **117**, 2134–2140.
8. Davies, J. and Cawley, P. The application of synthetic focusing for imaging crack-like defects in pipelines using guided waves. *IEEE Trans. Ultrason. Ferroel. Freq. Control*, 2009, **56**, 759–771.
9. Davies, J. and Cawley, P. The Application of synthetically focused imaging techniques for high resolution guided wave pipe inspection. In *Review of Progress in Quantitative NDE* (Thompson, D. and Chimenti, D., eds), (Plenum, New York, 2007), vol. 25, 681–688.
10. ABAQUS6.5. *Analysis User's Manual*. Abaqus, 2004.

Pikipragude avastamine ja visualiseerimine torudes ultrahelilainete abil

Madis Ratassepp, Sam Fletcher ja Aleksander Klauson

Ultrahelilained on leidnud torude kontrollimisel ulatuslikku rakendamist, kuna see meetod võimaldab kiiresti testida pikki toru lõike toru ühest punktist.

Samas on sellel tehnoloogial veel kitsaskohti defektide täpsel positsioneerimisel ja iseloomustamisel lainelevi keeruka käitumise tõttu. Selles uuringus kasutatakse defektide visualiseerimise meetodit, et avastada torudes pikipragusid. Visualiseerimine on vajalik, et määrata defekti täpne asukoht ja parandada defektilt peegeldunud signaalide amplituudi. Selleks kasutatakse ultrahelilainete sünteetilist fokuseerimist, mis võimaldab saada infot defekti kujutisest toru pinnal. Kasutades lõplike elementide modelleerimise andmeid, uuritakse kujutise amplituudi sõltuvalt prao pikkusest ja sagedusest nii läbivate kui ka mitteläbivate pragude juhul. Sondeerivaks laineks on väändelaine T(0,1). Tulemused näitavad, et mittefokuseerimise tehnikatega võrreldes suurendab fokuseerimine pikipragude avastamise tundlikkust. Siiski võimaldab meetodi tundlikkus avastada ainult väga sügavaid pragusid.